

# Heat pump driven by the shot noise of a tunnel contact

Robert Hussein<sup>a</sup>, Sigmund Kohler<sup>a</sup>, Fernando Sols<sup>b,\*</sup>

<sup>a</sup>*Instituto de Ciencia de Materiales de Madrid, CSIC, Cantoblanco, E-28049 Madrid, Spain*

<sup>b</sup>*Departamento de Física de Materiales, Facultad de Ciencias Físicas, Universidad Complutense de Madrid, E-28040 Madrid, Spain*

---

## Abstract

We investigate a mechanism for cooling a lead based on a process that replaces hot electrons by cold ones. The central idea is that a double quantum dot with an inhomogeneous Zeeman splitting acts as energy filter for the transported electrons. The setup is such that hot electrons with spin up are removed, while cold electrons with spin down are added. The required non-equilibrium condition is provided by the capacitive coupling of one quantum dot to the shot noise of a strongly biased quantum point contact in the tunnelling limit. Special attention is paid to the identification of an operating regime in which the net electrical current vanishes.

*Keywords:* quantum transport, heat exchange, cooling

---

## 1. Introduction

The program of devising novel refrigeration schemes for electronic systems defines a variety of fundamental problems of potential technological interest. The pumping of heat from a cold to a hot electron reservoir by suitably manipulating the electron transport may be viewed as a form of rectified motion [1, 2, 3]. Electron pumps can be adiabatic [4, 5, 6] or (if they use inelastic transitions) nonadiabatic [7, 8]. The latter case represents a particular instance of ac-driven electron heat transport [9, 10]. It has been recognized that the effect of nonadiabatic driving can be very similar to that of an energetic, far-from-equilibrium energy source that promotes inelastic transmission of electrons through a spatially asymmetric setup [11, 12, 13, 14]. In this paper, we follow the approach of these works and investigate the possible use of the shot noise of a nearby quantum point contact (QPC) as the nonequilibrium energy source that, through capacitive coupling, induces rectification in a spatially asymmetric device which in our case will be a double quantum dot (DQD) system.

In mesoscopic physics, recent experimental progress in energy harvesting [15] turned the fundamental issue of heat balance into a topic of practical interest [16]. In particular, quantum dot setups have been argued to provide a convenient framework for the controlled transport of heat between electron reservoirs [7, 12, 17, 18], as has been experimentally confirmed [19]. On the other hand, it has also been argued that capacitive coupling to systems with fluctuating charges can be a source of energy and of induced heat transport [20], a claim that has been recently observed [21]. A similar prediction for quantum

cavity systems [22] has also received experimental confirmation [23, 24]. Analogous physics has been predicted for small electron systems interacting through the exchange of phonons [25] or microwave photons [26]

When considering electron exchange between reservoirs, one typically assumes each lead in a grand canonical state determined by its chemical potential and its temperature. Then thermal excitations involve occupied states above the Fermi energy and unoccupied states below. Our focus lies on the associated excitation energies. Consequently, we speak of cooling when electrons in states above the Fermi energy are removed or when holes below are filled. Thus, one way to cool a lead is to contact it with another lead at a different chemical potential while applying an appropriate energy filter which can be realized, e.g., by the gap of a superconductor [27] or by a resonant level. The same principle can be applied to the cooling of of a two-dimensional electron gas mediating the charge flow between two leads, as has been predicted [28] and observed [29]; for a review see [30]. A recent experiment is presented in Ref. [31], which is based on the mechanism proposed in Ref. [20].

The above cooling scheme, however, relies on an applied bias which also causes a net electron transfer. In particular when one lead is actually a small grain, one soon reaches a situation in which the grain becomes electrically charged and the cooling process comes to an end. In this article we follow Ref. [7] by proposing a mesoscopic heat pump that avoids a net charge transport while operating between two leads with equal chemical potentials. In consistency with the second law of thermodynamics, such a heat flow from cold to hot requires some non-equilibrium condition. In Ref. [7], this has been theoretically achieved by an gating. Here by contrast, we employ the shot noise of a nearby quantum point contact. The shot noise of a nearby

---

\*Corresponding author

Email address: [f.sols@fis.ucm.es](mailto:f.sols@fis.ucm.es) (Fernando Sols)

conductor has already been investigated as a source of rectification [32, 33, 34]. Here we adapt the study in Ref. [34], where the fluctuating conductors is a QPC in the tunnel limit, to the pumping of heat with zero net electric current between the cold and the hot leads. The advantage of using a charge-fluctuating QPC is two-fold: First, its broad-band excitation is less sensitive to small detunings. Second, most recent quantum dots already include such a QPC [35, 36] so that our proposal can be realized readily.

The behavior of quantum dot systems subject to the effect of nearby fluctuations can be studied as a particular case of the “particle-bath” problem, where attention is paid to the effect on a few physical variables (or on a reduced Hilbert space) of many degrees of freedom that are mathematically traced out [37]. The effect of the dissipative environment is that of rendering the dynamics effectively irreversible despite the time-reversal symmetry of the underlying microscopic dynamics. On a macroscopic level, irreversibility becomes manifest in the fact that heat can flow spontaneously only from a hot to a cold reservoir. Such a quantum dissipation approach underlies the master equation calculation described in section 2, where the leads degrees of freedom are traced out.

This paper is arranged as follows. In section 2 we describe the model considered and the calculation method employed. Section 3 contains analytical and numerical results for the case of noninteracting electrons. In section 4, we discuss the effect of Coulomb repulsion at the dots, focusing on the displacement of the particle-hole symmetry point. Section 5 is devoted to conclusions. Appendix A provides a detailed account of the arguments leading to the analytical results obtained for the charge and heat currents which are presented in section 3.

## 2. Model and master equation

### 2.1. DQD coupled to a QPC in the tunnel regime

Our model sketched in Fig. 1 consists of two capacitively coupled electric circuits, namely an unbiased DQD and a strongly biased tunnel contact. The latter entails non-equilibrium noise on the former and, thus, drives the DQD out of equilibrium. The DQD is modeled by the Hamiltonian

$$H_{\text{DQD}} = \frac{\Omega}{2} \sum_{\sigma=\uparrow,\downarrow} (c_{1\sigma}^\dagger c_{2\sigma} + c_{2\sigma}^\dagger c_{1\sigma}) + \frac{U}{2} \sum_{\kappa \neq \kappa'} n_\kappa n_{\kappa'} + \sum_{i=1,2} B_i (c_{i\uparrow}^\dagger c_{i\uparrow} - c_{i\downarrow}^\dagger c_{i\downarrow}) + V_{\text{gate}} \sum_{\kappa} c_\kappa^\dagger c_\kappa \quad (1)$$

where  $i = 1, 2$  and  $\sigma = \uparrow, \downarrow$  label the two quantum dots and the spin degree of freedom, respectively, while the multi index  $\kappa = (i, \sigma)$  combines both. The terms describe spin-independent tunneling  $\Omega$ , Coulomb repulsion  $U$ , an inhomogeneous Zeeman splitting  $B_i > 0$ , and a global shift of the onsite energies caused by a background gate voltage (with the sign convention that a positive  $V_{\text{gate}}$  shifts

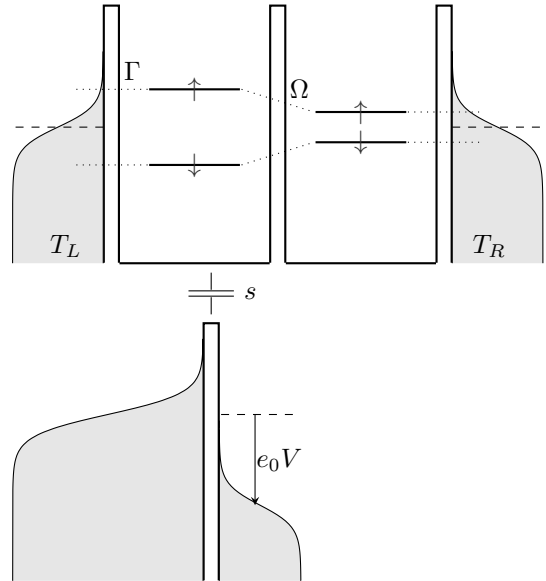


Figure 1: Sketch of the double quantum dot (DQD) coupled to a QPC in the tunnel regime. We focus on the heat balance in the right lead of the DQD, where hot spin-up electrons are removed while cold spin-down electrons are added. The coupling to the shot noise of the QPC creates a non-equilibrium situation that breaks the symmetry between the forward and the backward process. In the absence of the QPC, detailed balance inhibits cooling.

the DQD levels upwards). For simplicity, we restrict ourselves to undetuned dot levels (in the absence of the magnetic field) and assume that both intra-dot and inter-dot Coulomb repulsion are equal.

Dot 1 is tunnel coupled to the left lead  $L$  described by  $H_{\text{dot-lead}} = \sum_{q,\sigma} \epsilon_q (c_{L,q,\sigma}^\dagger c_{1,\sigma} + c_{1,\sigma}^\dagger c_{L,q,\sigma})$  and dot 2 accordingly to the right lead. The effective dot-lead coupling is given by the rate  $\Gamma = 2\pi \sum_q |V_{L,q}|^2 \delta(\epsilon - \epsilon_q)$  which we assume independent of the energy  $\epsilon$  and the spin projection  $\sigma$ . Then the equilibrium distribution of the lead electrons is given by the Fermi function  $f_\ell(\epsilon) = [\exp(\epsilon/k_B T_\ell) + 1]^{-1}$  where  $\ell = L, R$ , i.e., while setting  $\mu = 0$  for both leads, we allow for different lead temperatures

Our second system is a QPC in the tunnel limit between two leads modeled by the Hamiltonian  $H_{\text{QPC}} = \sum_k \epsilon_k c_k^\dagger c_k + \sum_{k'} \epsilon_{k'} c_{k'}^\dagger c_{k'}$ , where  $k$  and  $k'$  label the modes of the left and the right lead, respectively, including the spin. The leads are weakly coupled by the tunnel Hamiltonian  $\Lambda = \Lambda_+ + \Lambda_-$ , where

$$\Lambda_+ = \sum_{k,k'} t_{kk'} c_k^\dagger c_{k'}, \quad (2)$$

transfers an electron from the left to the right QPC lead, while  $\Lambda_- \equiv \Lambda_+^\dagger$  describes the opposite process. In the continuum limit, the matrix elements  $t_{kk'}$  are encompassed by the energy-independent QPC conductance  $G = 2\pi \sum_{kk'} |t_{kk'}|^2 \delta(\epsilon - \epsilon_k) \delta(\epsilon - \epsilon_{k'})$  in units of the conductance quantum  $G_0 = e_0^2/h$ . The electrons on dot 1 enhance, via Coulomb repulsion, the barrier between the QPC leads and thereby reduce the tunnel matrix elements

$t_{kk'}$ . This effect is captured by a prefactor  $x = (1 - sn_1)$  in the tunnel Hamiltonian such that

$$H_{\text{QPC}}^{\text{tun}} = x(\Lambda_+ + \Lambda_-) \quad (3)$$

accounts for both the QPC and its coupling to the DQD. The latter is mediated by the occupation of dot 1,  $n_1 = \sum_{\sigma} n_{1\sigma}$ . For consistency, the dimensionless coupling  $s$  must obey  $0 \leq s \leq 1/2$ .

## 2.2. Master equation

Our theoretical description is based on the formal elimination of all four leads such that we remain with a reduced master equation for the DQD. While the treatment of the leads coupled to the DQD follows a standard procedure, the systematic elimination of the tunnel contact is less common and has been performed only recently [38, 34]. In those works, a counting variable for the tunnel contact allowed to compute the full counting statistics and correlation functions, while here it is sufficient to compute the action of the QPC on the DQD. We sketch here the derivation of the formalism of Ref. [38, 34] as required for our present purposes.

We start from the Liouville-von Neumann equation for the full density operator which we transform to the interaction picture with respect to  $H_{\text{DQD}}$  and the lead Hamiltonians. The remaining terms are treated within second-order perturbation theory in the dot-lead tunnelings and in the QPC tunneling to obtain the Bloch-Redfield master equation [39]

$$\dot{\rho} = -\frac{i}{\hbar}[H_S, \rho] - \frac{1}{\hbar^2} \sum_n \int_0^{\infty} dt \text{tr}_{\text{leads}}[V_n, [\tilde{V}_n(-t), \rho \otimes R_0]], \quad (4)$$

for the reduced DQD density operator  $\rho$ .  $R_0$  refers to the grand canonical ensemble of each lead, while the operators  $V_n$  represent  $H_{\text{QPC}}^{\text{tun}}$  and the two tunnel contributions in  $H_{\text{DQD-leads}}$ . Here,  $\tilde{V}_n(t)$  stands for  $V_n$  in the interaction picture.

The evaluation of the Liouvillian  $\mathcal{L}_{\text{DQD-leads}}$  for the incoherent DQD-lead tunneling is rather standard, see e.g. the appendix of Ref. [40]. It yields operators that describe jumps between many-particle DQD states differing by one electron. The transition rates contain Fermi functions reflecting the initial occupation of the lead modes. To obtain an expression for the heat balance, we multiply in the superoperator for the electric current each tunnel process by the energy with respect to the chemical potential which the electron carries to the lead [41, 9, 7, 10].

To obtain the Liouvillian for the action of the QPC, we evaluate the  $t$ -integral in Eq. (4) and find the QPC Liouvillian

$$\mathcal{L}_{\text{QPC}}\rho = \frac{1}{2\hbar^2} \int_{-\infty}^{+\infty} dt C(t) [\tilde{x}(-t)\rho x + x\rho\tilde{x}(t) - x\tilde{x}(-t)\rho - \rho\tilde{x}(t)x]. \quad (5)$$

Symmetrizing the time integral amounts to neglecting the energy renormalization stemming from principal values. A main ingredient is the correlation function of the QPC tunnel operator,  $C(t) = \langle \Lambda(t)\Lambda(0) \rangle = C_+(t) + C_-(t)$ , where  $C_{\pm}(t) = \langle \Lambda_{\mp}(t)\Lambda_{\pm}(0) \rangle$  is readily evaluated from its definition and the assumption that the leads are voltage biased. In Fourier representation it reads [42]

$$C_{\pm}(\omega) = G \frac{\hbar\omega \pm e_0V}{1 - \exp[-(\hbar\omega \pm e_0V)/k_B T]}. \quad (6)$$

We restrict ourselves to the limit in which the QPC bias  $V$  is much larger than any other relevant frequency scale of the DQD. Then  $C(\omega) = \hbar e_0 G V$  becomes frequency independent so that  $C(t) \propto \delta(t)$ . Then we obtain for the QPC Liouvillian the Lindblad form

$$\mathcal{L}_{\text{QPC}}\rho = \gamma(x\rho x - [x^2, \rho]/2) \quad (7)$$

with the effective rate  $\gamma = 2\pi I_{\text{QPC}}/e_0$ . For a treatment beyond the large-bias limit, see Ref. [34].

In our numerical implementation of the master equation formalism, we use the many-particle eigenstates of the DQD Hamiltonian as a basis and keep all off-diagonal elements of the density matrix. This ensures to capture the level repulsion stemming from the tunnel coupling, which is rather relevant for levels close to the Fermi energy.

## 3. Heat balance in the absence of interaction

To explain the central idea of the cooling mechanism, we consider the channels for the spin-up electrons and for the spin-down electrons separately. To do so, we ignore Coulomb repulsion which couples the spin-up and the spin-down channels. Later we will see that the interaction term in the Hamiltonian (1) shifts the working point and affects the efficiency.

### 3.1. Pumping mechanism

We consider the DQD sketched in the upper half of Fig. 1. Let us focus on the channel for the spin-down electrons and assume equal temperatures,  $T_L = T_R$ . Suppose that an electron enters dot 1 from the left lead at the corresponding onsite energy. The electron may proceed to dot 2 and eventually to the right lead. Due to the lower occupation at higher initial energy, the opposite process occurs with lower probability. Thus we expect a net transport that in the right lead fills holes below the Fermi surface, which corresponds to cooling.

However, this picture is incomplete. Owing to the tunnel coupling between the dots, DQD eigenstates are delocalized, but in such a way that (spin-down) electrons in the ground state are mostly in the left dot while the excited ones dwell mostly in the right dot. Therefore, electrons in the excited states are more likely to leave to the right lead, while electrons preferentially enter the ground state from the left lead. The quantitative analysis [see Eqs. (8) and

(9) below] reveals that, when both leads have the same temperature and chemical potential, those processes fail to yield a net effect, i.e., both the electric current and the heat current vanish. This is of course what one expects for such an equilibrium situation. In more technical terms, the full description obeys detailed balance, as it should.

To obtain any net transport, we must drive the system out of equilibrium. For this purpose, we couple the DQD to a strongly biased QPC in the tunnel regime; see the Hamiltonian (3). Then the shot noise of the tunnel current induces transitions between the ground state and the excited state of the DQD. Since the ground state is more strongly populated, we witness a net excitation and, consequently, the transport process from left to right dominates the one in the opposite direction. We thus observe both charge pumping and cooling of the right lead.

The channel for the spin-up electrons behaves similarly. It yields a net transport of hot electrons from the right to the left lead, which again corresponds to cooling. In the symmetric situation  $V_{\text{gate}} = 0$  sketched in Fig. 1, the transported charges of both spin channels compensate each other, while the energy transfer adds up. The net result is cooling of the right lead without charge accumulation.

### 3.2. Quantitative analysis of the individual channels

In order to substantiate the above discussion, we have solved the master equation for a single spin channel within the rotating-wave approximation. This approximation means that, within a Pauli-type master equation approach, off-diagonal density matrix elements are neglected and only the populations of the eigenstates are considered. The QPC-induced transitions between the (single-particle) ground state and the excited state of the DQD have been treated as a perturbation. Moreover, we have ignored the doubly occupied state. While details of the calculation can be found in Appendix A, we present here the results for the electric current and the heat balance in the limit  $\gamma \ll \Gamma$ :

$$I = \frac{\gamma}{4} \frac{f_e - f_g}{1 - f_g f_e} \frac{\varepsilon \Omega^2}{(\varepsilon^2 + \Omega^2)^{3/2}}, \quad (8)$$

$$\dot{Q} = \frac{\gamma}{8} \frac{f_e - f_g}{1 - f_g f_e} \frac{\Omega^2}{(\varepsilon^2 + \Omega^2)^{1/2}} + (V_{\text{gate}} - \mu)I, \quad (9)$$

where  $\varepsilon$  is the Zeeman energy gradient,  $\varepsilon = (B_2 - B_1)/2$ , and the Fermi functions at the QDQ energies are abbreviated as  $f_g = f(E_g - \mu)$  and  $f_e = f(E_e - \mu)$ .

If the ground state lies well below the Fermi surface, so that  $f_g \simeq 1$ , while  $f_e$  is significantly smaller, the prefactor involving the Fermi functions becomes unity. Then both the electric current and the heat balance depend only on the DQD configuration and the distance to the symmetry point.

An important implication of Eqs. (8) and (9) is that both vanish in the absence of the QPC, since then  $\gamma = 0$ . This underlines that our treatment is consistent with detailed balance.

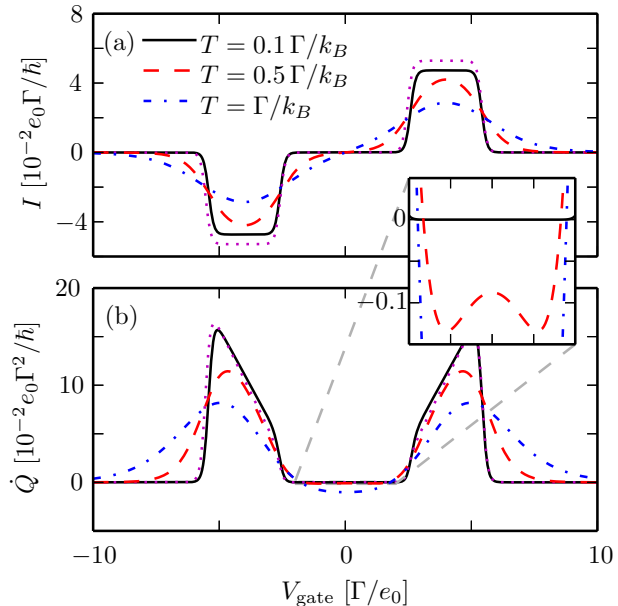


Figure 2: (a) Current and (b) heat balance as a function of the gate voltage  $V_{\text{gate}}$  for various DQD temperatures and zero Coulomb interaction. Parameters are  $\Gamma = 2\Omega = B_1/10 = B_2/6 = 2k_B T_{\text{QPC}} = \varepsilon_0 V/80$ , QPC conductance  $G = 1$ , and coupling strength  $s = 0.1$ . The dotted lines mark the analytical solution given in Appendix A, for  $k_B T = \Gamma/10$ . Inset: Zoom of the heat balance in the region close to  $V_{\text{gate}} = 0$  where  $\dot{Q} < 0$ .

### 3.3. Cooling

Our next goal is to provide numerical results for the different operating regimes. In doing so, we plot in Fig. 2 the electric current and the heat balance as a function of the gate voltage and for parameters that otherwise correspond to the sketch in Fig. 1.

For very negative gate voltage, all four levels lie below the Fermi surface and no transport occurs. When shifting all levels upwards, the excited state of the spin-up channel will cross the Fermi function and a pump current from the right to the left lead sets in. The initial energy of the corresponding electrons in the right lead is far below the Fermi surface. Therefore the creation of holes corresponds to heating the right lead, which visible in the large positive value of  $\dot{Q}$  at  $V_{\text{gate}} = -5\Gamma$ . For less negative  $V_{\text{gate}}$ , the energy of the created holes is also less negative and  $\dot{Q}$  is diminished. Once the ground state also lies above the Fermi energy, the process comes to rest. For positive  $V_{\text{gate}}$ , the spin-down channel is active and adds hot electrons. While this leads to an opposite electric current, it also corresponds to heating.

For zero temperature, the borders between the different regions are sharp and both the current and the heat balance between the peaks vanish exactly. For larger temperatures, the curves smear out. While at  $V_{\text{gate}} = 0$ , the electric current must vanish for symmetry reasons, the heat balance assumes negative values (see inset of Fig. 2). This means that we find a cooling process in which hot electrons of the right lead are replaced by cold ones.

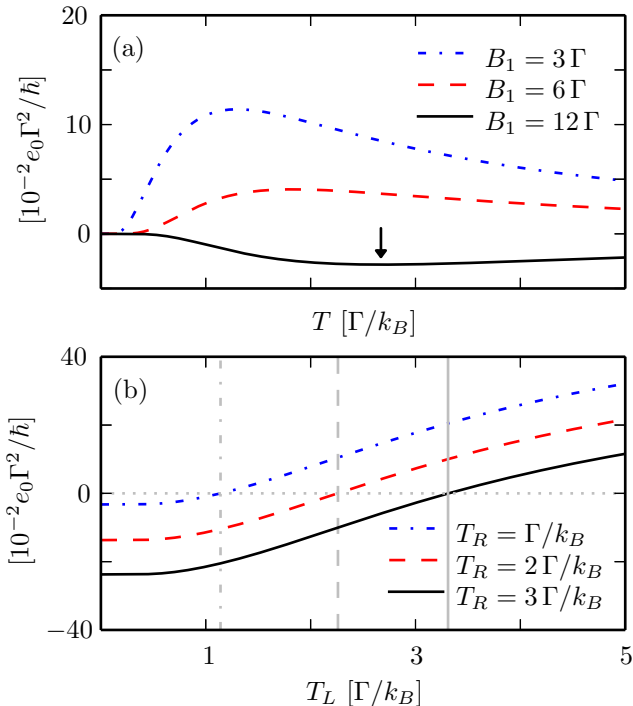


Figure 3: Heat current as a function of the temperature of the left lead for (a) equal temperatures  $T = T_L = T_R$  and (b) for pumping against a temperature gradient for various  $T_R$ . The Zeeman splitting in dot 2 is  $B_2 = 6\Gamma$ , while all other parameters are as in Fig. 2. The arrow in panel (a) marks the minimum of the curve for  $B_1 = 12\Gamma$ ; the vertical lines in panel (b) mark the zeros of the heat current and, therewith, the temperature up to which cooling can be achieved.

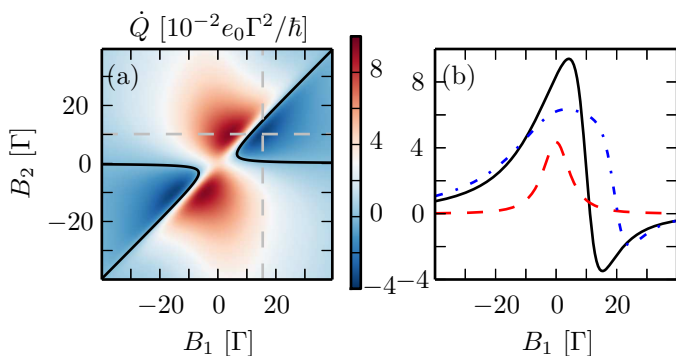


Figure 4: (a) Heat production rate on the right lead as a function of the Zeeman splittings  $B_1$  and  $B_2$  at the symmetry point for  $T = 3\Gamma/k_B$  and other parameters as in Fig. 2. The cross line indicates its minimum for positive Zeeman splittings. The solid contour line indicates vanishing heat current. (b) Corresponding slices at constant  $B_2 = 10\Gamma$  (solid line),  $B_2 = 20\Gamma$  (dashed), and  $B_2 = 30\Gamma$  (dashed-dotted).

Figure 3(a) shows the heat balance as a function of the temperature for different Zeeman splittings. Interestingly, at zero temperature,  $\dot{Q} = 0$  irrespective of the magnetic field gradient, i.e., not only the cooling but also the heating vanishes as expected. Moreover, the data indicate that cooling is possible only on the side on which the splitting is smaller. In the symmetric situation (dashed curve for  $B_1 = B_2$ ), we already observe significant heating in the right lead. For symmetry reasons it equals the heating of the left lead. Therefore, the coupling to the out-of-equilibrium QPC augments the total thermal energy, a behavior that agrees with our expectations.

A more systematic investigation of the magnetic field dependence is provided in Fig. 4. The overview as a function of  $B_1$  and  $B_2$  indicates that the optimal cooling of the right is found for  $B_2$  clearly smaller than  $B_1$ , but not too small. One might have expected that  $B_1$  should be as large as possible to ensure a strong population of the relevant states in the left lead. However, in such a case the onsite levels are strongly detuned so that the effective transition matrix element of the perturbation between the DQD eigenstates becomes small; see Appendix A.

A most intriguing question is whether one can reduce the thermal energy of one lead even when it is already at a lower temperature than the other lead, i.e., whether one can pump heat from cold to hot. In Fig. 3(b) we show the results for pumping heat against a temperature gradient. Globally, we find that this is possible for moderate temperature differences of roughly 10%.

#### 4. Coulomb repulsion

To make our study applicable to realistic quantum dots, we have to include Coulomb repulsion. For  $U = 0$ , we had chosen our working point at  $V_{\text{gate}} = 0$  where both channels are symmetric with respect to the Fermi energy. Therefore we start by writing the interaction term in the DQD Hamiltonian (1) in a more symmetric form with the help of the identity

$$\sum_{\kappa \neq \kappa'} n_{\kappa} n_{\kappa'} = \sum_{\kappa \neq \kappa'} \left( n_{\kappa} - \frac{1}{2} \right) \left( n_{\kappa'} - \frac{1}{2} \right) + (N-1) \sum_{\kappa} n_{\kappa} - \frac{1}{4} N(N-1), \quad (10)$$

where  $n_{\kappa} = c_{\kappa}^{\dagger} c_{\kappa}$  is the occupation of the single particle level  $\kappa = 1, \dots, N$ . The interpretation of this identity is that our interaction Hamiltonian can be expressed by the particle-hole symmetric terms  $c_{\kappa}^{\dagger} c_{\kappa} - 1/2 = -(c_{\kappa} c_{\kappa}^{\dagger} - 1/2)$  plus an onsite energy. To be specific, the interaction term in Eq. (1) is particle-hole symmetric if a gate voltage shifts the  $N = 4$  levels by  $-3U/2$  [recall the prefactor  $U/2$  in the interaction term of the Hamiltonian (1)].

The predicted shift of the operating point is indeed visible in the current and the heat balance as a function of the gate voltage and the interaction strength plotted in Fig. 5.

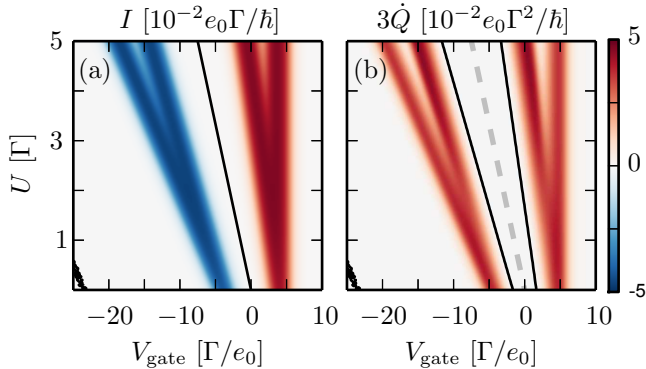


Figure 5: (a) Electric current and (b) heat balance as a function of the gate voltage  $V_{\text{gate}}$  and the Coulomb interaction  $U$  for  $k_B T = \Gamma/2$ . Other parameters are as in Fig. 2. Black contour lines indicate vanishing current and heat current, respectively. The grey dashed line,  $V_{\text{gate}} = -3U/2$ , in panel (b) marks the points for which the electric current is zero. That line tracks the particle-hole symmetry point which is displaced by the interaction.

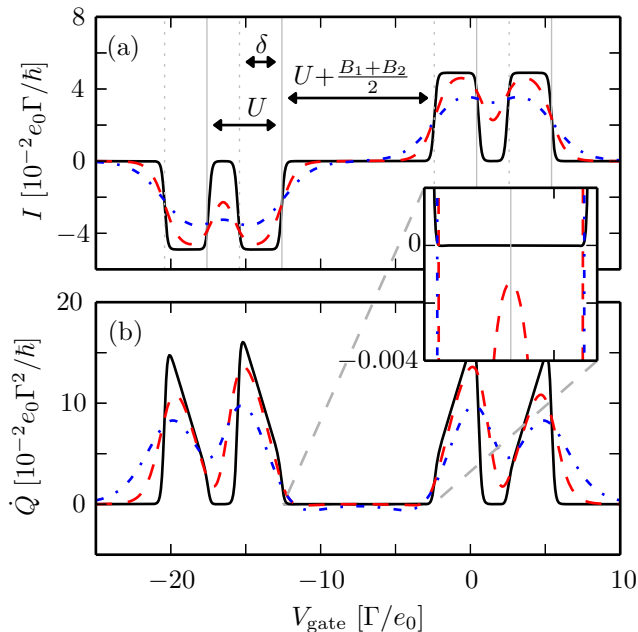


Figure 6: (a) Current and (b) heat current as function of the gate voltage  $V_{\text{gate}}$  as in Fig. 2 but for nonzero Coulomb interaction  $U = 5\Gamma$ . Vertical lines indicate the transition energies listed in Appendix A. Inset: Heat current in the region close to the symmetry point  $V_{\text{gate}} = -(3/2)U$  which is indicated by a vertical line.

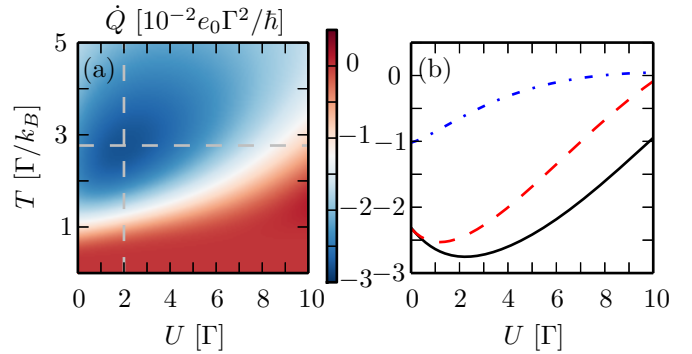


Figure 7: (a) Heat current on the right lead at the symmetry point, as a function of the DQD temperature and the Coulomb interaction for parameters as in Fig. 2. The cross line indicates its minimum. (b) Corresponding slices at constant  $T = 3\Gamma/k_B$  (solid line),  $T = 2\Gamma/k_B$  (dashed), and  $T = \Gamma/k_B$  (dashed-dotted).

The plot also reveals that with increasing interaction, each current peak splits into two peaks with a distance  $U$ . The values of these shifts can be appreciated in the horizontal slices of both panels shown in Fig. 6. The physical reason for the peak separation is that for each channel, the onsite energies are relevant for the empty channel, while for the occupation with a further electron, one must overcome the Coulomb repulsion. This effectively augments the excitations energies by  $U$ .

As a drawback, the interaction energy not only shifts the working point, but also changes  $\dot{Q}$  quantitatively. The data in Fig. 7 shows that the cooling effect has a maximum at finite  $U$  where the location of the optimum value depends on the temperature. Thus, small interactions may be beneficial for cooling, but with increasing  $U$ , the cooling power decays and may even turn into heating. Thus an experimental realization of our scheme should be attempted with quantum dots that have a large capacity.

## 5. Conclusions

We have shown that a double quantum dot subject to an asymmetric Zeeman splitting and capacitively coupled to the charge fluctuations of a nearby quantum point contact in the tunnel limit can experience rectification. In a suitable region of parameter space, the system can act as a heat pump that cools the lead coupled to the dot with the weaker Zeeman splitting, even if that lead is already the coldest one. Such a refrigeration scheme can operate with a zero net electric current across the double quantum dot system. This is possible thanks to a particle-hole symmetry that can be preserved if the gate voltage is suitably adjusted to compensate the effect of Coulomb repulsion. For this setup to act as a heat pump, electric current creating shot noise must flow through the nearby quantum point contact. However, that electric current does not need to run parallel to the line connecting the two heat reservoirs through the double quantum dot system. This feature can become an important advantage in potential applications.

## Acknowledgments

We would like to thank Rafael Sánchez for valuable comments. This work has been supported by Spain's MINECO under grants no. FIS2013-41716-P and MAT2014-58241-P.

## Appendix A. Analytical solution for an individual channel

Transport through an individual spin channel can be described by a Pauli-type rate equation  $\dot{P} = \mathcal{M}P$  for the occupation probabilities  $P = (P_0, P_g, P_e)^T$  in the energy basis  $|0\rangle|0\rangle, |g\rangle|g\rangle, |e\rangle|e\rangle$ . The ground and excited states are parametrized [43] by

$$|g\rangle = -\sin\theta|1\rangle + \cos\theta|2\rangle, \quad |e\rangle = \cos\theta|1\rangle + \sin\theta|2\rangle, \quad (\text{A.1})$$

where  $|1\rangle$  and  $|2\rangle$  refer to the left and right DQD state, respectively, in the local basis. The geometrical factors are determined by  $\cos(2\theta) = -\epsilon_\sigma/\delta$  and  $\sin(2\theta) = |\Omega|/\delta$ , with level splitting  $\delta = \sqrt{\epsilon_\sigma^2 + |\Omega|^2}$  and detuning

$$\epsilon_\sigma = \frac{B_1 - B_2}{2} \text{sgn}(\sigma), \quad (\text{A.2})$$

where  $\text{sgn}(\sigma)$  is positive for  $\sigma = \uparrow$  and negative, otherwise.

The Liouvillian reads

$$\mathcal{M} = \begin{bmatrix} -a-b & \bar{a} & \bar{b} \\ a & -\bar{a}-\gamma' & \gamma' \\ b & \gamma' & -\bar{b}-\gamma' \end{bmatrix}, \quad (\text{A.3})$$

where  $a = \Gamma - \bar{a} = \Gamma f(E_g - \mu)$  and  $b = \Gamma - \bar{b} = \Gamma f(E_e - \mu)$  are finite dot-lead tunneling rates. Albeit the leads are in equilibrium, electrons can still be excited by the driving of the QPC, which is modeled by Fermi's golden rule rate  $\gamma' = (s/2)^2 \sin^2(2\theta) C(-\delta)$  of the coupling operator  $H_{\text{QPC}}^{\text{tun}}$ . From the current operator

$$\mathcal{J} = \begin{bmatrix} 0 & \bar{a} \sin^2(\theta) & \bar{b} \cos^2(\theta) \\ -a \sin^2(\theta) & 0 & 0 \\ -b \cos^2(\theta) & 0 & 0 \end{bmatrix}, \quad (\text{A.4})$$

and the heat current operator

$$\mathcal{J}_Q = \frac{\delta}{2} \begin{bmatrix} 0 & \bar{a} \sin^2(\theta) & -\bar{b} \cos^2(\theta) \\ -a \sin^2(\theta) & 0 & 0 \\ b \cos^2(\theta) & 0 & 0 \end{bmatrix}, \quad (\text{A.5})$$

follows directly the current  $I = \text{tr} \mathcal{J} P^{\text{st}}$  and the heat current  $\dot{Q} = \text{tr} \mathcal{J}_Q P^{\text{st}}$ , respectively. Hereby,  $\text{tr} = (1, 1, 1)$  denotes the trace operator and

$$P^{\text{st}} = \frac{1}{\Gamma^2 - ab + (2\Gamma + a + b)\gamma'} \begin{bmatrix} \bar{a}\bar{b} + (\bar{a} + \bar{b})\gamma' \\ \bar{a}\bar{b} + (a + b)\gamma' \\ \bar{a}\bar{b} + (a + b)\gamma' \end{bmatrix} \quad (\text{A.6})$$

the stationary state with  $\mathcal{M}P^{\text{st}} = 0$ . Finally, we obtain

$$I = \gamma' \Gamma \cos(2\theta) \frac{a-b}{\Gamma^2 - ab + (2\Gamma + a + b)\gamma'} = \frac{s^2 \Gamma C(-\delta)}{4} \frac{b-a}{\Gamma^2 - ab + (2\Gamma + a + b)\gamma'} \frac{\epsilon_\sigma |\Omega|^2}{\delta^3}, \quad (\text{A.7})$$

and

$$\begin{aligned} \dot{Q} &= -\frac{\delta}{2 \cos(2\theta)} I - (\mu - V_{\text{gate}}) I \\ &= \frac{s^2 \Gamma C(-\delta)}{8} \frac{b-a}{\Gamma^2 - ab + (2\Gamma + a + b)\gamma'} \frac{|\Omega|^2}{\delta} \\ &\quad + (V_{\text{gate}} - \mu) I. \end{aligned} \quad (\text{A.8})$$

The ground energy  $E_g$  and the excited energy  $E_e$  occurring in the Fermi functions are given by  $E_{g/e} = V_{\text{gate}} - E_{k,\sigma}^\pm$  with

$$E_{k,\sigma}^\pm = -kU \pm \delta/2 - \frac{B_1 + B_2}{4} \text{sgn}(\sigma). \quad (\text{A.9})$$

The latter includes a displacement by a multiple  $k$  of the Coulomb interaction. To emphasize explicitly the dependence on the spin  $\sigma$  and this multiple  $k$ , we write in the following the current of the individual channels as  $I = I_{k,\sigma}$ .

The two-channel case can be approximated by summation of the single-channel solutions for spin-up and spin-down. For vanishing Coulomb interaction, the two channel current is obtained from  $I_{0,\downarrow} + I_{0,\uparrow}$ , while it is composed of  $I_{0,\downarrow} + I_{1,\downarrow} + I_{2,\uparrow} + I_{3,\uparrow}$  for finite  $U \gg \delta$ . The analytical heat current for the two channels case can be analogously defined. The two channels case for vanishing Coulomb interaction is in Fig. 2 compared to the numerical solution of the full master equation. Further, figure 6 shows the transition energies for finite Coulomb interaction—the vertical lines, from left to right, are given by the energies  $E_{k,\sigma}^s$  at  $(k, \sigma, s) = (3, \uparrow, -), (3, \uparrow, +), (2, \uparrow, -), (2, \uparrow, +), (1, \downarrow, -), (1, \downarrow, +), (0, \downarrow, -), (0, \downarrow, +)$ .

## References

- [1] M. Büttiker, Transport as a consequence of state-dependent diffusion, *Z. Phys. B Condens. Matter* 68 (1987) 161.
- [2] P. Reimann, Brownian motors: Noisy transport far from equilibrium, *Phys. Rep.* 361 (2002) 57.
- [3] P. Hänggi, F. Marchesoni, Artificial brownian motors: Controlling transport on the nanoscale, *Rev. Mod. Phys.* 81 (2009) 387.
- [4] T. E. Humphrey, R. Newbury, R. P. Taylor, H. Linke, Reversible quantum brownian heat engines for electrons, *Phys. Rev. Lett.* 89 (2002) 116801.
- [5] J. E. Avron, A. Elgart, G. M. Graf, L. Sadun, Transport and dissipation in quantum pumps, *J. Stat. Phys.* 116 (2004) 425.
- [6] J. P. Pekola, F. Giazotto, O.-P. Saira, Radio-frequency single-electron refrigerator, *Phys. Rev. Lett.* 98 (2007) 037201.
- [7] M. Rey, M. Strass, S. Kohler, F. Sols, P. Hänggi, Nonadiabatic electron heat pump, *Phys. Rev. B* 76 (2007) 085337.
- [8] F. Chi, Y. Dubi, Microwave-mediated heat transport in a quantum dot attached to leads, *J. Phys.: Condens. Matter* 24 (2012) 145301.
- [9] M. Moskalets, M. Büttiker, Floquet scattering theory of quantum pumps, *Phys. Rev. B* 66 (2002) 205320.



- [10] L. Arrachea, M. Moskalets, L. Martin-Moreno, Heat production and energy balance in nanoscale engines driven by time-dependent fields, *Phys. Rev. B* 75 (2007) 245420.
- [11] J. P. Pekola, F. W. J. Hekking, Normal-metal-superconductor tunnel junction as a brownian refrigerator, *Phys. Rev. Lett.* 98 (2007) 210604.
- [12] D. Segal, Single mode heat rectifier: Controlling energy flow between electronic conductors, *Phys. Rev. Lett.* 100 (2008) 105901.
- [13] F. Sols, Aspects of quantum cooling in electron and atom systems, *Physica E* 42 (2010) 466.
- [14] B. Cleuren, B. Rutten, C. Van den Broeck, Cooling by heating: Refrigeration powered by photons, *Phys. Rev. Lett.* 108 (2012) 120603.
- [15] H. B. Radousky, H. Liang, Energy harvesting: an integrated view of materials, devices and applications, *Nanotechnology* 23 (2012) 502001.
- [16] B. Sothmann, R. Sánchez, A. N. Jordan, Thermoelectric energy harvesting with quantum dots, *Nanotechnology* 26 (2015) 032001.
- [17] R. Sánchez, B. Sothmann, A. N. Jordan, M. Büttiker, Correlations of heat and charge currents in quantum-dot thermoelectric engines, *New J. Phys.* 15 (2013) 125001.
- [18] D. Venturelli, R. Fazio, V. Giovannetti, Minimal self-contained quantum refrigeration machine based on four quantum dots, *Phys. Rev. Lett.* 110 (2013) 256801.
- [19] H. Thierschmann, M. Henke, J. Knorr, L. Maier, C. Heyn, W. Hansen, H. Buhmann, L. W. Molenkamp, Diffusion thermopower of a serial double quantum dot, *New J. Phys.* 15 (2013) 123010.
- [20] R. Sánchez, M. Büttiker, Optimal energy quanta to current conversion, *Phys. Rev. B* 83 (2011) 085428.
- [21] H. Thierschmann, R. Sánchez, B. Sothmann, F. Arnold, C. Heyn, W. Hansen, H. Buhmann, L. W. Molenkamp, Three-terminal energy harvester with coupled quantum dots, *Nature Nanotech* (2015) in press.
- [22] B. Sothmann, R. Sánchez, A. N. Jordan, M. Büttiker, Rectification of thermal fluctuations in a chaotic cavity heat engine, *Phys. Rev. B* 85 (2012) 205301.
- [23] B. Roche, P. Roulleau, T. Jullien, Y. Jompol, I. Farrer, D. Ritchie, D. Glatli, Harvesting dissipated energy with a mesoscopic ratchet, *Nature Commun.* 6 (2015) 6738.
- [24] F. Hartmann, P. Pfeffer, S. Höfling, M. Kamp, L. Worschech, Voltage fluctuation to current converter with coulomb-coupled quantum dots, *Phys. Rev. Lett.* 114 (2015) 146805.
- [25] O. Entin-Wohlman, Y. Imry, A. Aharony, Three-terminal thermoelectric transport through a molecular junction, *Phys. Rev. B* 82 (2010) 115314.
- [26] T. Ruokola, T. Ojanen, Theory of single-electron heat engines coupled to electromagnetic environments, *Phys. Rev. B* 86 (2012) 035454.
- [27] J. Pekola, Low-temperature physics: Tunnelling into the chill, *Nature* 435 (2005) 889.
- [28] H. L. Edwards, Q. Niu, G. A. Georgakis, A. L. de Lozanne, Cryogenic cooling using tunneling structures with sharp energy features, *Phys. Rev. B* 52 (1995) 5714.
- [29] J. R. Prance, C. G. Smith, J. P. Griffiths, S. J. Chorley, D. Anderson, G. A. C. Jones, I. Farrer, D. A. Ritchie, Electronic refrigeration of a two-dimensional electron gas, *Phys. Rev. Lett.* 102 (2009) 146602.
- [30] F. Giazotto, T. T. Heikkilä, A. Luukanen, A. M. Savin, J. P. Pekola, Opportunities for mesoscopics in thermometry and refrigeration: Physics and applications, *Rev. Mod. Phys.* 78 (2006) 217.
- [31] J. V. Koski, A. Kutvonen, T. Ala-Nissila, J. P. Pekola, On-chip Maxwell's demon as an information-powered refrigerator (2015) arXiv:1507.00530.
- [32] A. Levchenko, A. Kamenev, Coulomb drag in quantum circuits, *Phys. Rev. Lett.* 101 (2008) 216806.
- [33] R. Sánchez, R. López, D. Sánchez, M. Büttiker, Mesoscopic coulomb drag, broken detailed balance, and fluctuation relations, *Phys. Rev. Lett.* 104 (2010) 076801.
- [34] R. Hussein, S. Kohler, Capacitively coupled nano conductors: Ratchet currents and exchange fluctuation relations, *Ann. Phys. (Berlin)* (2015) in press; doi:10.1002/andp.201500141.
- [35] T. Ihn, S. Gustavsson, U. Gasser, B. Küng, T. Müller, R. Schleser, M. Sigrist, I. Shorubalko, R. Leturcq, K. Ensslin, Quantum dots investigated with charge detection techniques, *Solid State Commun.* 149 (2009) 1419.
- [36] D. Taubert, D. Schuh, W. Wegscheider, S. Ludwig, Determination of energy scales in few-electron double quantum dots, *Rev. Sci. Instrum.* 82 (2011) 123905.
- [37] A. O. Caldeira, A. L. Leggett, Quantum tunnelling in a dissipative system, *Ann. Phys. (N.Y.)* 149 (1983) 374.
- [38] R. Hussein, J. Gómez-García, S. Kohler, Monitoring quantum transport: Backaction and measurement correlations, *Phys. Rev. B* 90 (2014) 155424.
- [39] A. G. Redfield, On the theory of relaxation processes, *IBM J. Res. Develop.* 1 (1957) 19.
- [40] R. Hussein, S. Kohler, Coherent quantum ratchets driven by tunnel oscillations: Fluctuations and correlations, *Phys. Rev. B* 86 (2012) 115452.
- [41] U. Sivan, Y. Imry, Multichannel landauer formula for thermoelectric transport with application to thermopower near the mobility edge, *Phys. Rev. B* 33 (1986) 551.
- [42] G.-L. Ingold, Yu. V. Nazarov, Charge Tunneling Rates in Ultrasmall Junctions, Vol. 294 of NATO ASI Series B, Plenum, New York, 1992, p. 21.
- [43] T. Brandes, Coherent and collective quantum optical effects in mesoscopic systems, *Phys. Rep.* 408 (2005) 315.